HHS Public Access

Author manuscript

Int Urogynecol J. Author manuscript; available in PMC 2017 July 21.

Published in final edited form as:

Int Urogynecol J. 2016 February ; 27(2): 205–212. doi:10.1007/s00192-015-2804-8.

Assessment of urethral support using MRI-derived computational modeling of the female pelvis

Yun Peng[1], **Rose Khavari**[2], **Nissrine A. Nakib**[3], **Timothy B. Boone**[2], and **Yingchun Zhang**[1]

[1]Department of Biomedical Engineering, Cullen College of Engineering, University of Houston, Houston, Texas, USA 77204

[2]Department of Urology, Houston Methodist Hospital and Research Institute, Houston, TX, USA 77030

[3]Department of Urology, University of Minnesota, Minneapolis, MN, USA

Abstract

Introduction and Hypothesis—This study aims to assess the role of individual anatomical structures and their combinations to urethral support function.

Methods—A realistic pelvic model was developed from an asymptomatic female subject's MR images for dynamic biomechanical analysis using the finite element method. Validation was performed by comparing simulation results with dynamic MR imaging observations. Weaknesses of anatomical support structures were simulated by reducing their material stiffness. Urethral mobility was quantified by examining the urethral axis excursion from rest to the final state (Intra-abdominal pressure = 100cmH_2O). Seven individual support structures and five of their combinations were studied.

Result—Among seven urethral support structures, weakening the vaginal walls, puborectalis muscle and pubococcygeus muscle generated the top three largest urethral excursion angles. A linear relationship was found between urethral axis excursions and intra-abdominal pressure.

*Correspondence: Yingchun Zhang, Ph.D., Department of Biomedical Engineering, University of Houston, 2027 SERC Building, 3605 Cullen Blvd, Houston, TX 77024 USA, yzhang94@uh.edu, Telephone: 713-743-6127.

Conflict of Interest

Yun Peng	FINANCIAL DISCLAIMER/CONFLICT OF INTEREST: NONE
Rose Khavari	FINANCIAL DISCLAIMER/CONFLICT OF INTEREST: NONE
Nissrine A. Nakib	FINANCIAL DISCLAIMER/CONFLICT OF INTEREST: NONE
Timothy B. Boone	FINANCIAL DISCLAIMER/CONFLICT OF INTEREST: NONE
Yingchun Zhang	FINANCIAL DISCLAIMER/CONFLICT OF INTEREST: NONE

Authors' contribution

Yun Peng	Data collection; Manuscript writing
Rose Khavari	Project Development; Data collection
Nissrine A. Nakib	Project Development
Timothy B. Boone	Project Development; Manuscript writing
Yingchun Zhang	Project Development; Data collection; Manuscript writing

Weakening all three levator ani components together caused a larger weakening effect than the sum of each individually weakened component, indicating a nonlinearly-additive pattern. The pelvic floor responded to different weakening conditions distinctly: weakening the vaginal wall developed urethral mobility through collapsed vaginal canal while weakening the levator ani showed a more uniform pelvic floor deformation.

Conclusions—The computational modeling and dynamic biomechanical analysis provides a powerful tool to better understand the dynamics of the female pelvis under pressure events. The vaginal walls, puborectalis and pubococcygeus are the most important individual structures in providing urethral support. The levator ani muscle group provides urethral support in a well-coordinated way with a nonlinearly-additive pattern.

Keywords

Stress Urinary Incontinence; Magnetic Resonance Imaging; Pelvic Muscle; Urethral Hypermobility; Finite Element Method

Introduction

Lack of urethral support due to weakness in various components of the urethral support system (USS) has been considered as the main etiologic factor causing stress urinary incontinence (SUI) [1–3]. The “hammock hypothesis” describes support of the urethra by a coordinated action of fasciae and muscles, which provides a hammock onto which the urethra is compressed during increases in intra-abdominal pressure (IAP) [3]. In a broad sense, the USS includes the levator ani muscle, vaginal wall and connective tissues that are extrinsic to the urethra, as well as the coccygeus muscle, obturator internus muscle, piriformis muscle and pelvic organs such as the rectum and uterus, as all these structures reside in the female pelvis and interact intimately during pressure events to support the urethra.

Many studies have investigated the pathophysiology of SUI through medical imaging techniques such as ultrasonography [4], anatomical magnetic resonance (MR) imaging [5–7] and dynamic MR imaging [8–10]. To assess urethral hypermobility caused by isolated impairment of each specific USS component and to compare the components’ relative contribution to urethral support function would require the recruitment of patients with only one impairment condition, which is clinically challenging to identify clinically. Cross-subject differences in female pelvic floor anatomy also affect the objectivity of the comparison. Computer simulation using the finite element method (FEM) has been proven to be a useful tool due to its ability to conveniently simulate various impairment conditions and keep these comparisons based on the same subject, computer simulation using finite element method (FEM) has been proven a useful tool [11]. Several computer models developed from MR images have been reported recently in studies of female pelvic floor dysfunctions such as pelvic organ prolapse [12,13], childbirth related levator ani muscle damages [14,15] and ligament impairment [16]. However, the clinical application of these models and their comparisons to the true dynamic response of the pelvis is limited due to either 1) missing or simplified important anatomical structures (e.g., the bladder, rectum, vaginal canal, uterus are not included [14,15]; buffering fatty tissues are not included [12–

16]) or 2) less accurate realization of boundary conditions (e.g., direct inferior displacement is applied on the uterus [13]; intra-abdominal pressure is directly applied on the muscle [16] or vaginal wall [12] that are studied). A comprehensive pelvic model, which incorporates 44 anatomical structures in the female pelvis to maintain the integrity of the natural pelvic anatomy, was developed in this study to better understand the role of individual structures and their combination on urethral support in women.

Materials and Methods

A 21-year-old healthy female subject (nulliparous, non-smoker, BMI=22) was recruited according to a protocol approved by the Institutional Review Boards (IRBs) of the University of Minnesota and the University of Houston, for a high-resolution pelvic MRI scan in the supine position at rest with a 3T MRI scanner (Trio Tim, Siemens, Germany) (slice thickness 3mm; matrix 320 × 160; field of view 430mm; pixel size 1.344mm). For validation purposes, dynamic MR images were acquired in the mid-sagittal plane approximately every 1.5 second while the subject performed several Valsalva maneuvers.

Image segmentation was first performed on the axial MR images for each anatomical pelvic structure with the guidance of urologists using Mimics 11.0 (Materialise Group, Leuven, Belgium). The closed surfaces were reconstructed for each anatomical structure and exported in STL (Stereolithography) format. Those surfaces were imported into MAYA 8.5 (Autodesk, Inc., San Rafael, CA) and Rhinoceros 4.0 (McNeel North America, Seattle, WA) for artifact smoothing and intersecting surface correction and then converted into solid SAT (Standard ACIS Text) geometries. All solid geometries were discretized into finite element meshes with a total number of 126,378 tetrahedral elements in ABAQUS 6.12 (SIMULIA, Providence, RI). The final 3D pelvic model contains 44 anatomical parts including pelvic muscles, sphincteric muscles, ligaments, bones, fat, bladder, urethra, uterus, vagina, deep perineal pouch, colon, rectum and anus. In addition, a bodyfill part was created to fill the intra-abdominal space for pressure transmission. A stiff Q-tip swab part was placed in the urethra to simulate the Q-tip swab that has been frequently used in clinical diagnosis and research for SUI [17,18]. Figure 1 illustrates the reconstructed 3D pelvic model. The bottom of the model was restrained from both translations and rotations. Two uniformly distributed pressures were applied on the front and top surfaces of the bodyfill to simulate valsalva. The IAP was calculated as the averaged contact pressure between the urine and inner bladder wall.

Soft tissues involved in the pelvic model were modeled as linear elastic solids using material properties from Young's moduli of the bladder, urethra, uterus, rectum, muscle, ligament and vaginal tissue (0.05, 0.03, 0.05, 0.1, 2.4, 1.2 and 7.4e-3 *MPa*) [19,11]. A soft material (Young's modulus of 0.04 *MPa*) was assigned to the bodyfill part. Urine was modeled as an elastic liquid with a Young's modulus of 1.0e-3 *MPa*. All soft tissues were considered incompressible considering that they contain abundant water. The bony pelvis was modeled as one rigid and fixed structure considering its negligible deformation under normal pelvic functions due to its much higher stiffness compared with soft tissues [16,20]. A simplifying condition was made to not include the voluntary contraction of the pelvic muscles, as it is often the case that, unless the female is trained using pelvic floor physical therapy, the

female pelvic floor responds to acute increase of intra-abdominal pressure without voluntary contractions, such as during coughing or sneezing.

The general contact algorithm in ABAQUS was applied to mimic the natural interaction between parts that are in contact but anatomically independent, such as the bladder and uterus, the uterus and rectum, or the pelvic muscles and fatty tissues. Tie constraints in ABAQUS that binds two shared surfaces were used to couple motions of parts which are biologically connected (e.g., the coccygeus muscle and the coccyx) and to model the connecting effects of fasciae (e.g., the tendineous arch of levator ani muscle between the iliococcygeus muscle and the obturator internus muscle). Connector elements, with the ability to model connective tissues such ligaments [12], were employed in this study to model the uterosacral and cardinal ligaments. The Abaqus/Explicit solver was used for finite element method implementation.

A validation study was first performed by comparing the pelvic floor configurations achieved in computer simulation results with dynamic MR imaging observations along the mid-sagittal plane at both rest and maximal Valsalva maneuver (Figure 2). The subject was instructed on how to perform a Valsalva maneuver for the dynamic MR imaging and asked to hold each Valsalva maneuver for at least 2 seconds. During Valsalva maneuver, the abdominal muscles were contracted. Special attention was paid to the motions of the bladder, urethra, uterus and rectum. The results showed that the bladder, uterus and rectum slide in a posterior direction under the elevated IAP. It was also observed that the increased IAP led to bladder neck descent and clockwise rotation of the urethra, both of which are important landmarks commonly used in assessing urethral supports. The achieved consistency demonstrated the competence of the computer modeling and simulation method in characterizing pelvic floor responses to increased IAP.

The plan of simulation used in this study is listed in Table 1. The first two columns list the test numbers and weakened parts with their abbreviations in brackets. The impairment of each structure was simulated by reducing the elastic modulus by 90% [16]. Test00 serves as the asymptomatic control test based on the intact model in which no impairment was present. In each test from 01 to 07, a single USS component was weakened (hereafter referred to as single tests); in each test from 08 to 12, a specific group of USS components was weakened (hereafter referred to as group tests. Weakening the levator ani muscle was considered as a group test because the levator ani muscle group is composed of three individual muscle components. SUI is often associated with urethral hypermobility. Transperineal ultrasound reveals that the alpha-angle, defined as the angle between the vertical axis and the urethral axis [4], was significantly different on straining ($P<0.05$) between the study (SUI) and control groups. In this study, the alpha angle was monitored from the onset of the simulation to the final status, at which the IAP reached 100cmH_2O [21]. The urethral excursion angle, defined by the corresponding change in the α-angle ($\Delta\alpha$) and mathematically equal to the Q-tip excursion in clinical tests [18], was also monitored as an alternative metric to examine the urethral support function in this study. Since the α-angle at rest showed no significant difference ($P=0.650$) between SUI and control groups [4] and only the urethral support loss attributed to the weakness of specific anatomical structure(s) is

considered in this computation study, the static morphologic variation in the α-angle between asymptomatic and SUI subjects was not accounted for.

Linear regression analyses were performed for all curves (urethral excursion angles vs. intra-abdominal pressure) in MATLAB R2014 (Mathworks Inc., Natick, MA) using a linear model ($\Delta\alpha \sim k * IAP$). The interception of the linear model was set to zero considering that the urethral excursion angle should be zero at the onset of simulation (IAP = 0cmH_2O). The $\Delta\alpha$ achieved in the intact test (noted as $\Delta\alpha_{Intact}$) indicates the inherent response to the applied IAP of an asymptomatic USS. A weakening effect index ($WEI = \Delta\alpha - \Delta\alpha_{Intact}$) was also employed to elicit the degree of mobility caused solely by the weakened structure in each weakening test.

Results

The α-angle at the onset of simulation (at rest) was 15.9° for all tests. Table 1 shows the α-angles achieved at the final status with the IAP of 100cmH_2O for all tests. The final α-angles ranged from 30.3° (intact test) to 50.7° (weakened levator ani muscle and vaginal wall). The corresponding urethral excursion angles ($\Delta\alpha$) were calculated based on the difference between the onset and final α-angles (Table 1). The $\Delta\alpha_{Intact}$ reached 14.4° for the particular participant in this study. The results further showed that, $\Delta\alpha$ values were below 20° when only single pelvic muscle was weakened (from 15.3° to 19.4°). The vaginal wall, the puborectalis muscle and the pubococcygeus muscle were found to be the top three most contributing structures. Weakening these parts generated the top three largest urethral excursion angles ($\Delta\alpha$ = 20.1°, 19.4° and 18.8°, respectively), while weakening other muscles (the iliococcygeus, piriformis, coccygeus and obturator internus muscles) generated relatively smaller excursion angles ($\Delta\alpha$ < 17°). Weakening the levator ani muscle alone (test09) or in combination with other pelvic muscles (test10–12) raised the $\Delta\alpha$ value above 30°. The fitted R-square values for the urethral excursion angle-IAP curves (see Figure 3) fall into the range between 0.95 and 0.99, indicating a strong linear relationship between the urethral excursion angle and increased IAP for all the tests.

A nonlinearly-additive pattern was found among the three levator ani muscle components in terms of weakening effect ($WEI = \Delta\alpha - \Delta\alpha_{Intact}$). A WEI of 12.0° was achieved when weakening the puborectalis and pubococcygeus muscles together (test08), which is larger than the sum of WEIs achieved by weakening these two muscles separately (WEI = 5.0° in test05 and WEI = 4.4° in test06). The same nonlinear additive pattern was more remarkable by comparing the WEI obtained from weakening the entire levator ani muscle (WEI = 18.5°, test09) with the sum of WEIs from tests in weakening the three components weakened separately (WEI = 1.4° in test02, WEI = 5.0° in test05 and WEI = 4.4° in test06). Such a pattern did not exist for combinations of the levator ani muscle with other muscle groups (test10, 11 and 12). This finding suggests that the levator ani muscle is a sophisticated structure which provides support to the urethra in a well-coordinated fashion.

Distinct deformation patterns were found in the pelvic floor responses under different weakening conditions (see Figure 4). When the vaginal tissues were weakened, an observation was made that the vaginal canal underwent severe compression and the vaginal

wall became extremely thin, yielding more space for extra urethral motions, while the shape and position of the levator ani muscle did not show evident difference. However, when the levator ani muscle was weakened, a different pattern was observed: the vaginal wall remained at its normal thickness, while the levator ani muscle showed remarkable backward and downward yielding especially in the mid-portion, as the combinational effect of the front and top pressures applied on the bodyfill part on the entire pelvic floor is similar to a body force that is oriented in the inferoposterior direction and perpendicular to the levator plate. The urethral axis excursion in this case was attributed more to the insufficient support by the weakened levator ani muscle rather than the collapsed vaginal canal. When the levator ani muscle and the vaginal wall were both weakened simultaneously, both syndromes could be identified.

Discussion

Our female pelvic model consisting of 44 anatomical structures to mimic the dynamic response to pressure events represents, to the best of our knowledge, the most comprehensive and complete pelvic model in female SUI research. The validation study demonstrated consistency between the computer simulation results and the dynamic MR imaging observations along the sagittal plane of the pelvis of the same subject. A parametric study was designed and performed to investigate the relative importance of individual structures or their combination on urethral support in women. The α-angles from our computer simulations are in agreement with findings from transperineal ultrasound [4].

The relationship between the IAP and the induced urethral hypermobility may vary widely across subjects due to differences in anatomy and the functional status of the urethral support system [22]. However, simultaneous examination of these two metrics may provide useful information for a standardized evaluation of the functional status of the female pelvis. A significant association ($p=0.012$) between the ratio of IAP over Q-tip angle (urethral mobility index) and the degree of cystourethrocele was reported in a study that involved with eighty-four incontinence women [23]. The authors proposed this urethral mobility index as a standardized index for crossing-subject comparison. Although it is often intuitively assumed that the extent of urethral hypermobility should be positively related to IAP, this is the first time that this relationship has shown to be linear. The linear relationship over the entire IAP range identified in this study provided a substantialized ground for the application of the urethral mobility index as this index could be obtained consistently at any IAP level with less vulnerability to IAP variations. Moreover, it could provide a comprehensive functional profile of the female pelvic floor to discern urethral mobility indices specific to each weakening condition. Any anatomical (such as mid-urethral sling surgery) or functional (e.g., enhanced pelvic muscle strength) change in the pelvis could also be simulated in the computational model to provide valuable references in pre-surgery planning, training, or other SUI treatment options.

In our model, the weakening effect is mild when only one single structure is weakened, consistent with Crystle et al. who found patients with good urethral support to have a rotation angle of less than 20° [17]. This finding reveals that the female USS is a stable system and could still provide sufficient support to the urethra under mild impairment.

Considering the Q-tip excursion >30° as a criteria for urethral hypermobility [17,18], we find that weakening the entire levator ani muscle (comprised of the iliococcygeus, puborectalis and pubococcygeus muscles) caused more urethral mobility and could possibly result in urethral hypermobility ($\Delta\alpha$ = 32.9°). This is consistent with the clinical observation that female SUI patients with urethral hypermobility are often associated with damages in the levator ani muscle [24].

Medical imaging techniques such as MRI or ultrasound have been widely used for diagnosis of SUI characterized by urethral hypermobility, but their application is limited to cases where morphologic defects of urethral support structures are main causes. However, the impairment is not always morphologically observable. Reduced stiffness in pelvic muscle [25], ligament and vaginal wall tissues due to aging or trauma [26] could also be associated with insufficient support. The computational modeling and biomechanical approach provides a useful tool for those cases where there is no imaging evidence of morphologic abnormalities in the USS. Moreover, with the capability to reproduce the pelvic floor deformation under different weakening scenarios and exporting dynamic or static landmarks of interest, our model could be employed to establish a subject-specific SUI profile that manifests the deformation pattern uniquely associated with each possible weakening scenario. The functional status of the urethral support structure could then be assessed by comparing the imaging finding with the established profile. The distinct deformation patterns under different weakening conditions provide valuable references for subject-specific SUI diagnosis, which would be difficult to obtain from other methods considering the particularly challenging requirement of the same patient to develop different weakening syndromes successively as well as the difficulty in capturing the extremely instantaneous dynamic deformation.

The computational modeling and biomechanical analysis approach presented in this study could also be employed to develop, design and optimize interventional treatment approaches/devices such as mid-urethral slings. The results under different weakening conditions provided in our model could be valuable in simulating worst case scenarios and determining the safety factor for sling products. Kociszewski et al. [27] showed that the success and complication rates of the sling surgery were highly associated with the implant position. Our model could also be used as a pre-surgery planning tool to reduce potential postoperative complications and improve treatment success rate on a subject-specific basis.

Limitations of this study are discussed below. First, this study lacks statistical information as our model was built based on one subject-specific anatomy. The subject-specific modeling approach provides a tool for personalized diagnosis and treatment outcome prediction for a specific patient. Analyses will be performed in the future based on the results from a group of patients to provide statistical information. Second, the pelvic model currently relies on the high-resolution MR images, which remains a relatively expensive procedure (approximately $500/MRI scan). The modeling procedure also takes about 1–2 weeks for experienced engineers and radiologists. A possible solution to make this approach more accessible is to build a pelvic model template based on the features of the patient group and use subject-specific ultrasound images for model modification. Another limitation, commonly shared by many other pelvic models, is that the voluntary contraction of muscles is not realized in the

pelvic model. To do so it would require a non-trivial finite element implementation technique as well as critical physiological calibrations for different levels of voluntary pelvic floor muscle contractions. Very recently, an advanced voluntary pelvic model was proposed and provides a way to model voluntary muscle contractions [28]. Nevertheless, the parameters associated with the voluntary muscle model were not obtained from actual voluntary contraction experiments in this study. A specially designed transvaginal and a transrectal high-density surface EMG probe, along with the internal muscle activity imaging technique [29,30], were recently developed in our group. We are currently using high-density surface EMG measurements to quantitatively characterize voluntary contractions of muscles in the female pelvis to further improve our pelvic modeling approach.

In conclusion, a comprehensive computational model of the female pelvis was reconstructed. The vaginal wall, puborectalis muscle and pubococcygeus muscle were found as the top three most important urethral support structures. Some unique patterns of the female pelvic floor deformation were identified, which indicate that the computational modeling and dynamic biomechanical analysis approach presents a powerful tool for female SUI research and clinical diagnosis. It could be potentially employed for subject-specific SUI evaluation and pre-surgery planning.

Acknowledgments

This work was supported in part by NIH 4R00DK082644, NIH K99DK082644 and the University of Houston. The authors would like to thank Dr. John O. DeLancey from the University of Michigan for his valuable consultation. The authors also would like to thank Mr. Thomas Potter for editing the manuscript.

References

1. Pirpiris A, Shek K, Dietz H. Urethral mobility and urinary incontinence. Ultrasound in Obstetrics & Gynecology. 2010; 36(4):507–511. [PubMed: 20503229]
2. Schick E, Jolivet-Tremblay M, Tessier J, Dupont C, Bertrand PE. Observations on the function of the female urethra: III: An overview with special reference to the relation between urethral hypermobility and urethral incompetence. Neurourology and urodynamics. 2004; 23(1):22–26. [PubMed: 14694452]
3. Delancey JOL. STRUCTURAL SUPPORT OF THE URETHRA AS IT RELATES TO STRESS URINARY-INCONTINENCE - THE HAMMOCK HYPOTHESIS. American Journal of Obstetrics and Gynecology. 1994; 170(6):1713–1723. [PubMed: 8203431]
4. Sendag F, Vidinli H, Kazandi M, Itil IM, Askar N, Vidinli B, Pourbagher A. Role of perineal sonography in the evaluation of patients with stress urinary incontinence. The Australian & New Zealand journal of obstetrics & gynaecology. 2003; 43(1):54–57. [PubMed: 12755349]
5. Fielding JR, Dumanli H, Schreyer AG, Okuda S, Gering DT, Zou KH, Kikinis R, Jolesz FA. MR-based three-dimensional modeling of the normal pelvic floor in women: quantification of muscle mass. American Journal of Roentgenology. 2000; 174(3):657–660. [PubMed: 10701604]
6. Kim JK, Kim YJ, Choo MS, Cho K-S. The urethra and its supporting structures in women with stress urinary incontinence: MR imaging using an endovaginal coil. American Journal of Roentgenology. 2003; 180(4):1037–1044. [PubMed: 12646452]
7. Lockhart ME, Fielding JR, Richter HE, Brubaker L, Salomon CG, Ye W, Hakim CM, Wai CY, Stolpen AH, Weber AM. Reproducibility of Dynamic MR Imaging Pelvic Measurements: A Multi-institutional Study 1. Radiology. 2008; 249(2):534–540. [PubMed: 18796659]
8. Del Vescovo R, Piccolo CL, Della Vecchia N, Giurazza F, Cazzato RL, Grasso RF, Zobel BB. MRI role in morphological and functional assessment of the levator ani muscle: use in patients affected

by stress urinary incontinence (SUI) before and after pelvic floor rehabilitation. European journal of radiology. 2014; 83(3):479–486. DOI: 10.1016/j.ejrad.2013.11.021 [PubMed: 24373837]

9. El Sayed RF, El Mashed S, Farag A, Morsy MM, Abdel Azim MS. Pelvic Floor Dysfunction: Assessment with Combined Analysis of Static and Dynamic MR Imaging Findings 1. Radiology. 2008; 248(2):518–530. [PubMed: 18574134]
10. RINNE K, Kainulainen S, Aukee S, Heinonen S, Nilsson CG. Dynamic magnetic resonance imaging of the behavior of the mid-urethra in healthy and stress incontinent women. Acta obstetricia et gynecologica Scandinavica. 2010; 89(3):373–379. [PubMed: 20113196]
11. Zhang Y, Kim S, Erdman AG, Roberts KP, Timm GW. Feasibility of using a computer modeling approach to study SUI induced by landing a jump. Annals of biomedical engineering. 2009; 37(7): 1425–1433. [PubMed: 19415493]
12. Luo J, Chen L, Fenner DE, Ashton-Miller JA, DeLancey JO. A multi-compartment 3-D finite element model of rectocele and Its interaction with cystocele. Journal of Biomechanics. 2015
13. Chen Z-W, Joli P, Feng Z-Q, Rahim M, Pirró N, Bellemare M-E. Female patient-specific finite element modeling of pelvic organ prolapse (POP). Journal of Biomechanics. 2014
14. Jing D, Ashton-Miller JA, DeLancey JO. A subject-specific anisotropic visco-hyperelastic finite element model of female pelvic floor stress and strain during the second stage of labor. Journal of biomechanics. 2012; 45(3):455–460. [PubMed: 22209507]
15. Parente MPL, Jorge RMN, Mascarenhas T, Fernandes AA, Martins JAC. Deformation of the pelvic floor muscles during a vaginal delivery. International Urogynecology Journal. 2008; 19(1):65–71. DOI: 10.1007/s00192-007-0388-7
16. Brandão S, Parente M, Mascarenhas T, da Silva ARG, Ramos I, Jorge RN. Biomechanical study on the bladder neck and urethral positions: Simulation of impairment of the pelvic ligaments. Journal of Biomechanics. 2015; 48(2):217–223. http://dx.doi.org/10.1016/j.jbiomech.2014.11.045. [PubMed: 25527889]
17. Crystle CD, Charme LS, Copeland WE. Q-TIP TEST IN STRESS URINARY INCONTINENCE. Obstetrics and Gynecology. 1971; 38(2):313. [PubMed: 5105346]
18. Ghoniem G, Stanford E, Kenton K, Achtari C, Goldberg R, Mascarenhas T, Parekh M, Tamussino K, Tosson S, Lose G. Evaluation and outcome measures in the treatment of female urinary stress incontinence: International Urogynecological Association (IUGA) guidelines for research and clinical practice. International Urogynecology Journal. 2008; 19(1):5–33.
19. Egorov V, van Raalte H, Lucente V. Quantifying vaginal tissue elasticity under normal and prolapse conditions by tactile imaging. International urogynecology journal. 2012; 23(4):459–466. [PubMed: 22072417]
20. Dalstra M, Huiskes R, Odgaard A, van Erning L. Mechanical and textural properties of pelvic trabecular bone. Journal of Biomechanics. 1993; 26(4–5):523–535. http://dx.doi.org/10.1016/0021-9290(93)90014-6. [PubMed: 8478354]
21. Cobb WS, Burns JM, Kercher KW, Matthews BD, Norton HJ, Heniford BT. Normal intraabdominal pressure in healthy adults. Journal of Surgical Research. 2005; 129(2):231–235. [PubMed: 16140336]
22. Brandt FT, Lorenzato FR, Nobrega LV, Albuquerque CD, Falcao R, Araujo AA Junior. Intra-abdominal pressure measurement during ultrasound assessment of women with stress urinary incontinence: a novel model. Acta cirurgica brasileira/Sociedade Brasileira para Desenvolvimento Pesquisa em Cirurgia. 2006; 21(4):237–241.
23. Alafraa, T., Schick, E. Relation between Intra-abdominal pressure variation and urethral hypermobility: the urethral mobility index. Poster Abstract at International Continence Society; 2008.
24. DeLancey JOL. Fascial and muscular abnormalities in women with urethral hypermobility and anterior vaginal wall prolapse. American Journal of Obstetrics and Gynecology. 2002; 187(1):93–98. http://dx.doi.org/10.1067/mob.2002.125733. [PubMed: 12114894]
25. Verelst M, Leivseth G. Force and stiffness of the pelvic floor as function of muscle length: A comparison between women with and without stress urinary incontinence. Neurourology and urodynamics. 2007; 26(6):852–857. [PubMed: 17563104]

26. Chantereau P, Brieu M, Kammal M, Farthmann J, Gabriel B, Cosson M. Mechanical properties of pelvic soft tissue of young women and impact of aging. International urogynecology journal. 2014; 25(11):1547–1553. [PubMed: 25007897]

27. Kociszewski J, Rautenberg O, Kolben S, Eberhard J, Hilgers R, Viereck V. Tape functionality: position, change in shape, and outcome after TVT procedure—mid-term results. International urogynecology journal. 2010; 21(7):795–800. [PubMed: 20204326]

28. Brandão, FSQdS, Parente, MPL., Rocha, PAGG., Saraiva, MTdQeCdM, Ramos, IMAP., Natal Jorge, RM. Modeling the contraction of the pelvic floor muscles. Computer Methods in Biomechanics and Biomedical Engineering (ahead-of-print). 2015:1–10.

29. Liu Y, Ning Y, Li S, Zhou P, Rymer WZ, Zhang Y. Three-dimensional Innervation Zone Imaging from Multi-channel Surface EMG Recordings. International Journal of Neural Systems. 2015 In Press.

30. Yang L, Yong N, Jinbao H, Sheng L, Ping Z, Yingchun Z. Internal muscle activity imaging from multi-channel surface EMG recordings: A validation study. Conference proceedings: Annual International Conference of the IEEE Engineering in Medicine and Biology Society IEEE Engineering in Medicine and Biology Society Annual Conference. 2014; 2014:3559–3561. DOI: 10.1109/embc.2014.6944391

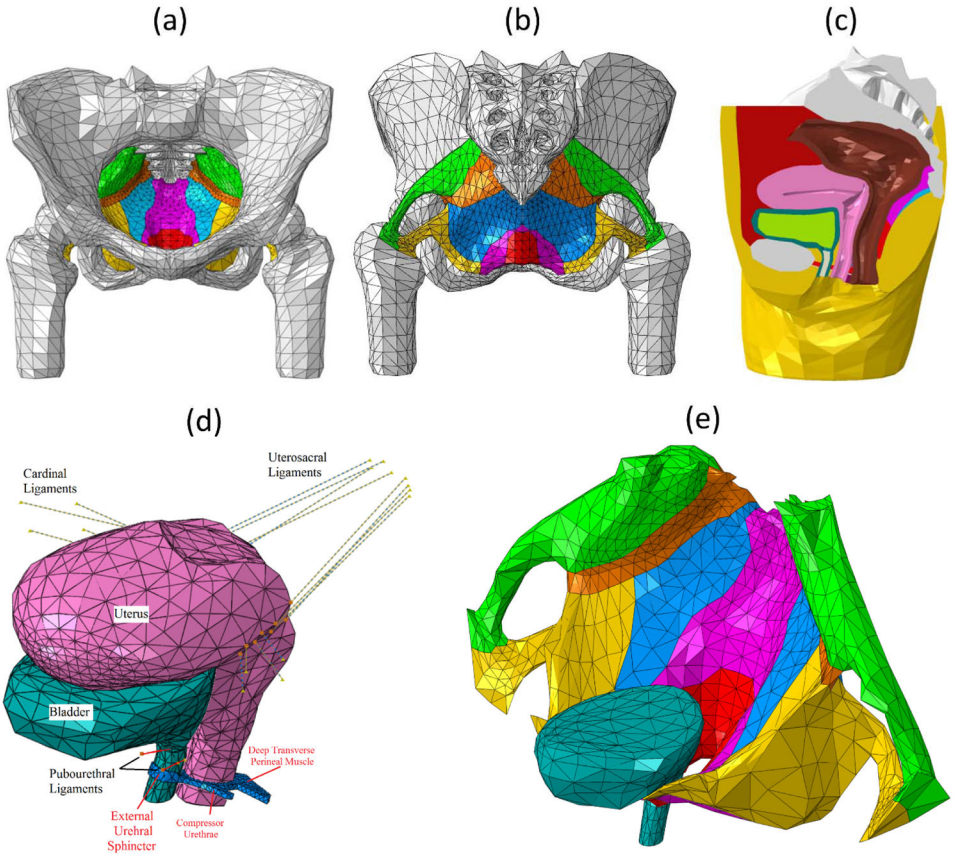

Figure 1.

(a) Front and (b) back view of all pelvic muscles, ligaments and bones (Fats and organs hidden for better visualization). (c) Mid-sagittal view of the entire pelvic model. (d) Anterior and posterior supports to urethra from pubourethral ligament, vagina and perineal pouch muscles. Ligaments were modeled using connector elements. The uterosacral ligaments attach the cervix to the posterior pelvic wall. The cardinal ligaments attach the cervix to the lateral pelvic wall. The pubourethral ligaments attach the bladder neck to the symphysis pubis. (e) Posterior support to urethra from pelvic floor muscles. In (a) (b) and (e), muscles are shown in different colors (green: piriformis, orange: coccygeus, blue: iliococcygeus, yellow: obturator Internus, magenta: pubococcygeus, red: puborectalis)

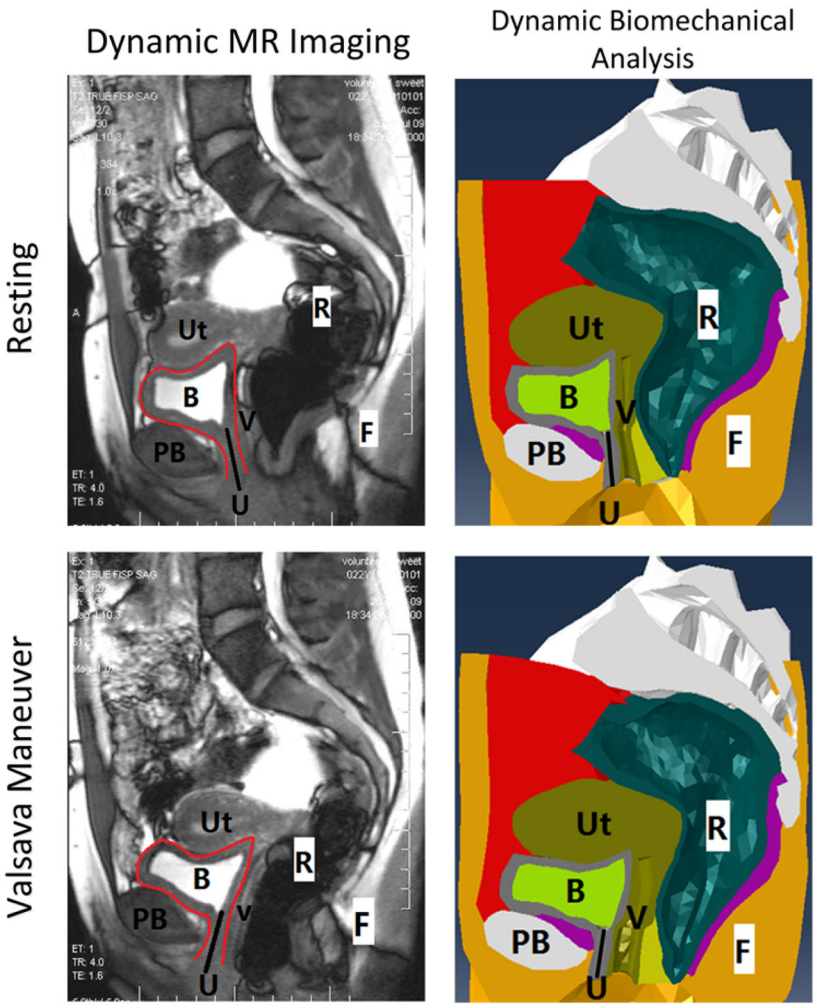

Figure 2.

Comparison (dynamic MR imaging vs. dynamic biomechanical analysis) of the pelvic structures of the female subject in the sagittal plane, at resting stage and at Valsalva stage. The black solid line in all pictures shows the location of urethra. The red curves in the dynamic MRI outline the bladder. (Abbreviations: Ut - Uterus, R - Rectum, B - Bladder, PB - Pubic Bone, V - Vagina, F - Fat, U - Urethra.)

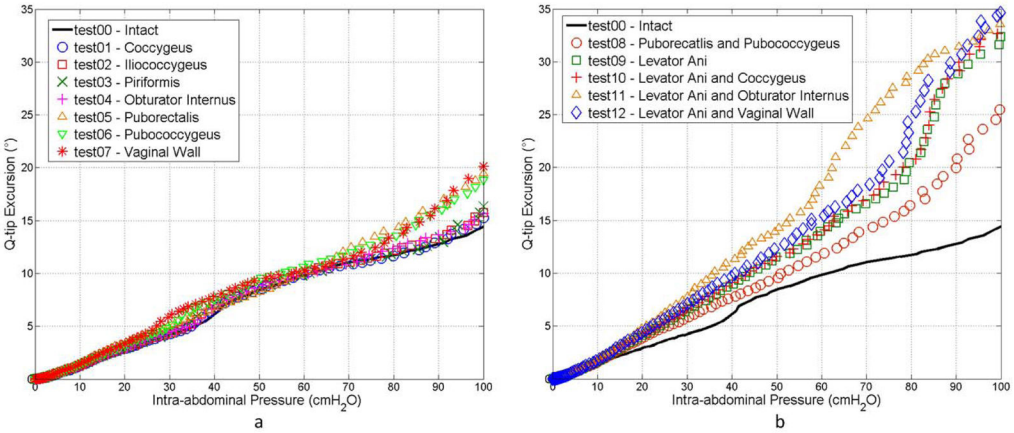

Figure 3.

Plots of urethral excursion angle against intra-abdominal pressure for (a) single tests and (b) group tests.

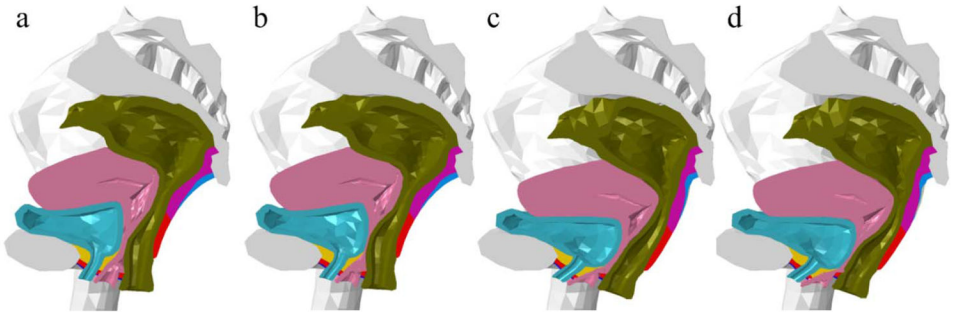

Figure 4.
Deformation patterns of (a) intact test (b) weakened vaginal wall (c) weakened levator ani muscle and (d) weakened levator ani muscle together with vaginal wall.

Table 1

Simulation Plan and Results

Test #	Weakened Part (Abbreviation)	α-angle (°) at IAP=100cmH_2O	Q-tip Excursion Δα (°)	Weakening Effect Index WEI = Δα − $\Delta\alpha_{intact}$ (°)
00	None	30.3	14.4 ($\Delta\alpha_{Intact}$)	0.0
Single Tests				
01	Coccygeus Muscle (CM)	31.1	15.3	0.8
02	Iliococcygeus Muscle (ICM)	31.6	15.8	1.4
03	Piriformis Muscle (PM)	32.2	16.3	1.9
04	Obturator Internus Muscle (OIM)	31.5	15.6	1.2
05	Puborectalis Muscle (PRM)	35.3	19.4	5.0
06	Pubococcygeus Muscle (PCM)	34.7	18.8	4.4
07	Vaginal Wall (VW)	36.0	20.1	5.7
Group Tests				
08	PRM + PCM	42.2	26.4	12.0
09	PRM+PCM+ICM = Levator Ani Muscle (LAM)	48.8	32.9	18.5
10	LAM + CM	49.0	33.2	18.8
11	LAM + OIM	50.0	34.1	19.7
12	LAM + VW	50.7	34.9	20.4

α-angle = 15.9° at rest for all tests)